

Text S1. Chemicals

The target contaminant metronidazole (MNZ), and other organic pollutants carbamazepine (CBZ, $\geq 98\%$), sulfamethoxazole (SMX, $\geq 98\%$), nitrobenzene (NB, 99%) were purchased from Adamas-beta[®] of China. Peroxymonosulfate (PMS, $\text{KHSO}_5 \cdot 0.5\text{KHSO}_4 \cdot 0.5\text{K}_2\text{SO}_4$), sodium chloride (NaCl , $\geq 99.0\%$), sodium dihydrogen phosphate (Na_2HPO_4 , $\geq 99.0\%$), sodium bicarbonate (NaHCO_3 , $\geq 99.0\%$), sodium sulphate (Na_2SO_4 , $\geq 99.0\%$), hydrochloric acid (HCl), 5,5-dimethyl-1-pyrrolidine-N-oxide (DMPO), 2,2,6,6-tetramethyl-4-piperidinyloxy (TEMP), and scavengers tertbutyl alcohol (TBA, $\geq 99.5\%$), furfuryl alcohol (FFA, $\geq 98\%$) and L-Histidine were also obtained from Adamas-beta[®] of China. sodium hydroxide (NaOH), sulfuric acid (H_2SO_4) and ethanol were obtained from Chengdu Kelong chemical reagent factory (Chengdu, China). 2,2-azino-bis(3-ethylbenzothiazoline)-6-sulfonic acid diammonium (ABTS, 99%) was purchased from Sigma-Aldrich China. All the reagents were of analytical grade and used without further purification. All solutions were prepared with ultrapure water.

Text S2. HPLC analysis of different compounds

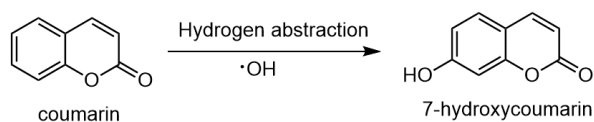
metronidazole (MNZ), sulfamethoxazole (SMX), carbamazepine (CBZ), nitrobenzene (NB), benzoic acid (BA), *p*-hydroxybenzoic acid (*p*-HBA) and *p*-benzoquinone (*p*-BQ) were measured using high performance liquid chromatography (HPLC, 1260 Infinity, Agilent, USA) equipped with the ultraviolet detector and the fluorescence detector. Other parameters were listed in Table S1.

Text S3. Determination of PMS concentration

The PMS concentration was measured by an UV-vis spectrometer (UV-3600, Shimadzu, Japan). Firstly, 10 mmol·L⁻¹ of 2,2-azino-bis(3-ethylbenzothiazoline)-6-sulfonic acid diammonium (ABTS) and 10 mmol·L⁻¹ of cobalt sulfate (Co(II)) were prepared before reaction. Sample (1ml) was taken in 10 mL cuvette at specified time intervals and topped to 10 mL with ultrapure water. And then, 0.4 mL 10 mmol·L⁻¹ of ABTS and 0.2 mL 10 mmol·L⁻¹ Co(II) were added. After shaking for 20 min, the absorbance was measured at $\lambda = 735$ nm by an UV-vis spectrometer and the PMS concentration was calculated using a standard curve method.

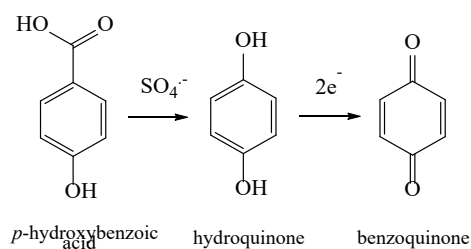
Text S4. Identification of hydroxyl radical ($\cdot\text{OH}$)

The concentration of 7-hydroxycoumarin (7-HC) was analyzed on high performance liquid chromatography (HPLC) (Prominence RF-20A, Shimadzu, Japan) equipped with a fluorescence (FLR) detector and a reverse-phase C18 column (4.6 \times 150 mm). The mobile phase composition was methanol/0.1% ammonium acetate (50:50, v/v). The flow rate and 1 mL/min and the temperature of liquid chromatographic column was 30 $^{\circ}\text{C}$. The fluorescence intensity was measured using a FLR detector with excitation wavelength of 346 nm and detection wavelength of 456 nm.



Text S5. Identification of sulfate radical ($\text{SO}_4^{\bullet-}$)

The $\text{SO}_4^{\bullet-}$ in reaction system was detected based on the method of indirect detection of *p*-benzoquinone (BQ), which is the major product of reaction between $\text{SO}_4^{\bullet-}$ and *p*-hydroxybenzoic acid (*p*-HBA). First, $1.8 \text{ mmol}\cdot\text{L}^{-1}$ *p*-HBA was added in the system. Sample was taken in the intervals specified after filtration by $0.22 \mu\text{m}$ polyether sulfone membranes. *p*-HBA and BQ were detected by HPLC (1260 Infinity, Agilent, USA) equipped with a DAD detector. The isometric elution was carried out with 50% pure water and 50% acetonitrile at a flow rate of $1 \text{ mL}/\text{min}$. The column temperature was set at 30°C . The absorption wavelength of *p*-HBA and BQ is 246 nm .



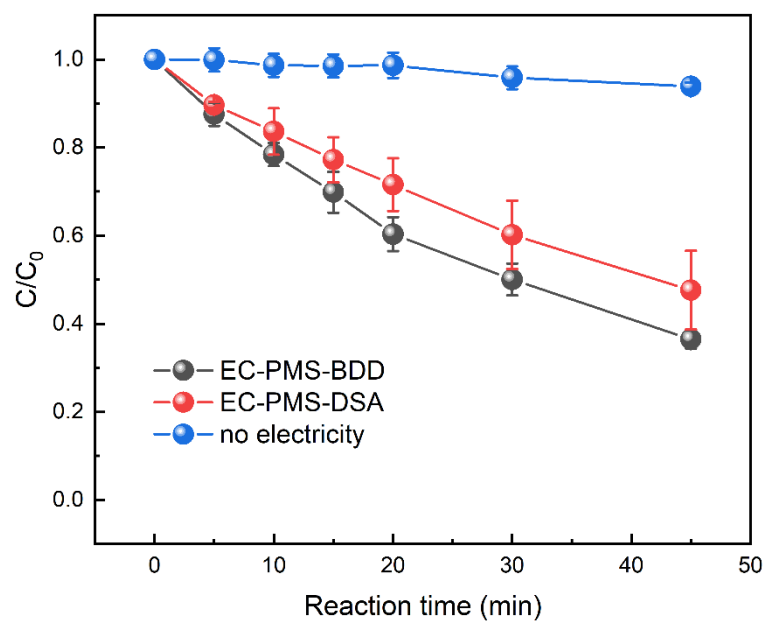


Figure S1. The concentration of PMS in EC-PMS-BDD and EC-PMS-DSA system. Reaction conditions: $[MNZ] = 80 \mu\text{mol}\cdot\text{L}^{-1}$, $[Na_2SO_4] = 20 \text{ mmol}\cdot\text{L}^{-1}$, $\text{pH}_0 = 6$, $I = 33.3 \text{ mA}/\text{cm}^2$.

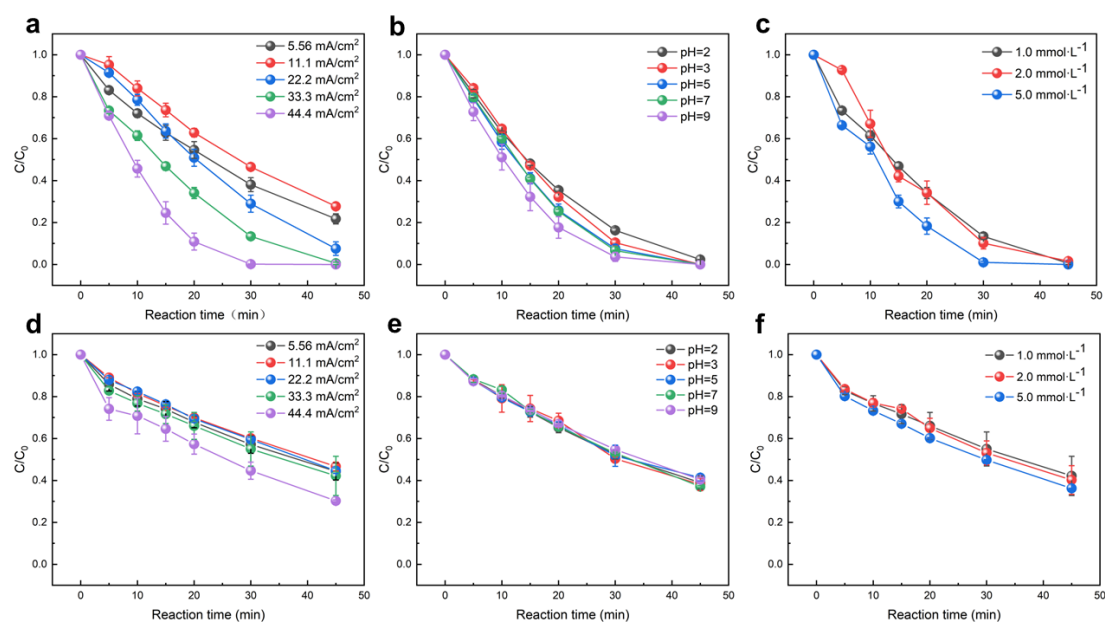


Figure S2. Effect of (a) current density, (b) initial pH, (c) PMS dosage on MNZ removal in EC-PMS-BDD system; effect of (d) current density, (e) initial pH, (f) PMS dosage on MNZ removal in EC-PMS-DSA system. Reaction conditions: $[MNZ] = 80 \mu\text{mol}\cdot\text{L}^{-1}$, $[Na_2SO_4] = 20 \text{ mmol}\cdot\text{L}^{-1}$, $pH_0 = 6$, $[PMS] = 1 \text{ mmol}\cdot\text{L}^{-1}$, $I = 33.3 \text{ mA}/\text{cm}^2$.

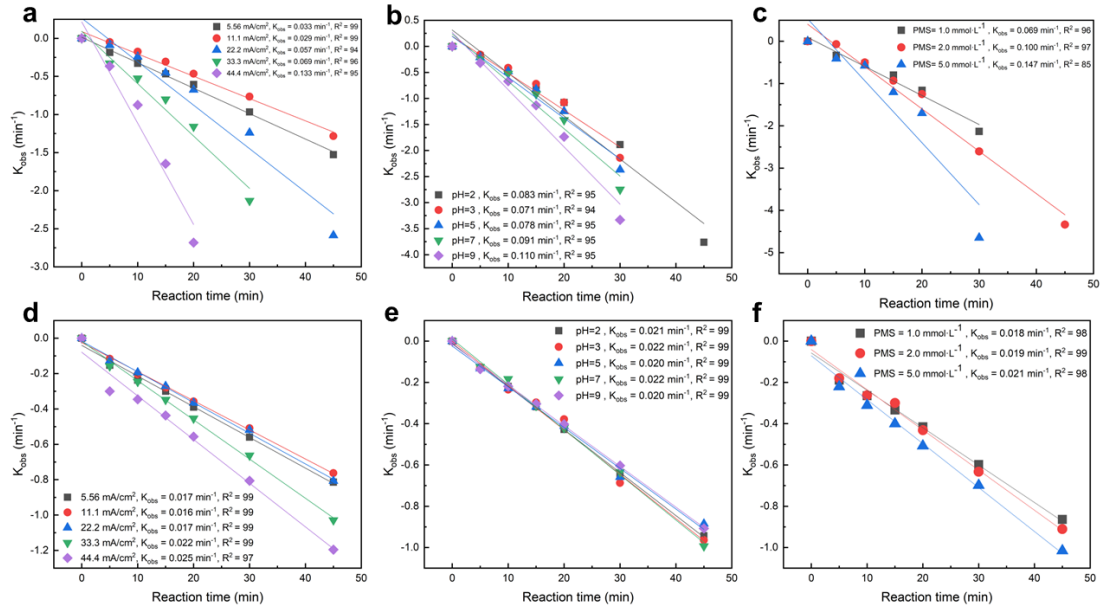


Figure S3. The pseudo-first-order kinetics model on MNZ degradation of (a) current density, (b) initial pH, (c) PMS dosage in EC-PMS-BDD process; the pseudo-first-order kinetics model on MNZ degradation of (d) current density, (e) initial pH, (f) PMS dosage in EC-PMS-DSA process. Reaction conditions: $[MNZ] = 80 \mu\text{mol}\cdot\text{L}^{-1}$, $[Na_2SO_4] = 20 \text{ mmol}\cdot\text{L}^{-1}$, $pH_0 = 6$, $[PMS] = 1 \text{ mmol}\cdot\text{L}^{-1}$, $I = 33.3 \text{ mA}/\text{cm}^2$.

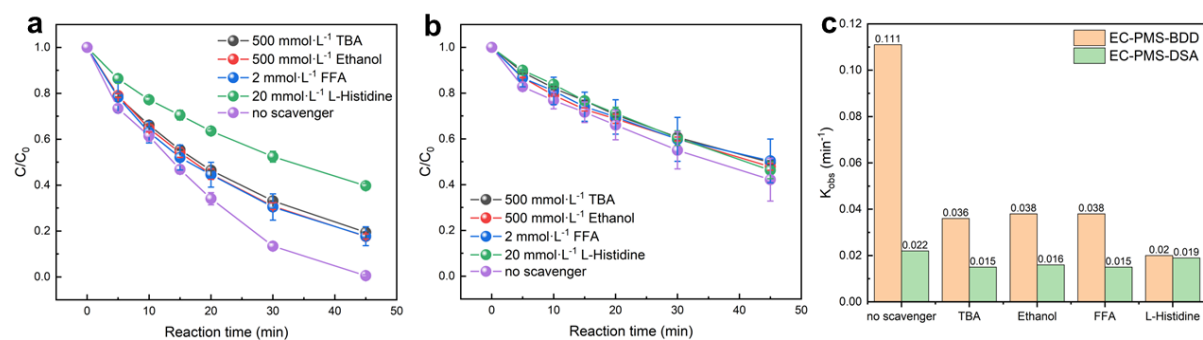


Figure S4. Effects of TBA, Ethanol, FFA and L-Histidine on MNZ removal efficiency in (a) EC-PMS-BDD process and (b) EC-PMS-DSA process; (c) Pseudo-first-order kinetic constant under different scavengers in EC-PMS-BDD and EC-PMS-DSA process.

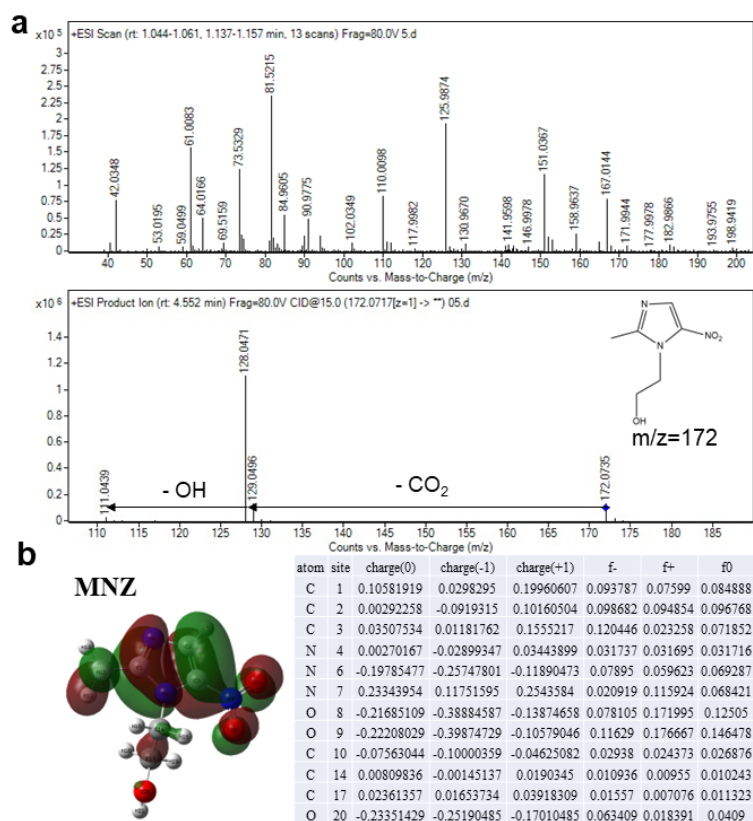


Figure S5. (a) Identification of MNZ (m/z +172) and its fragment ions, and (b) the Fukui index of MNZ.

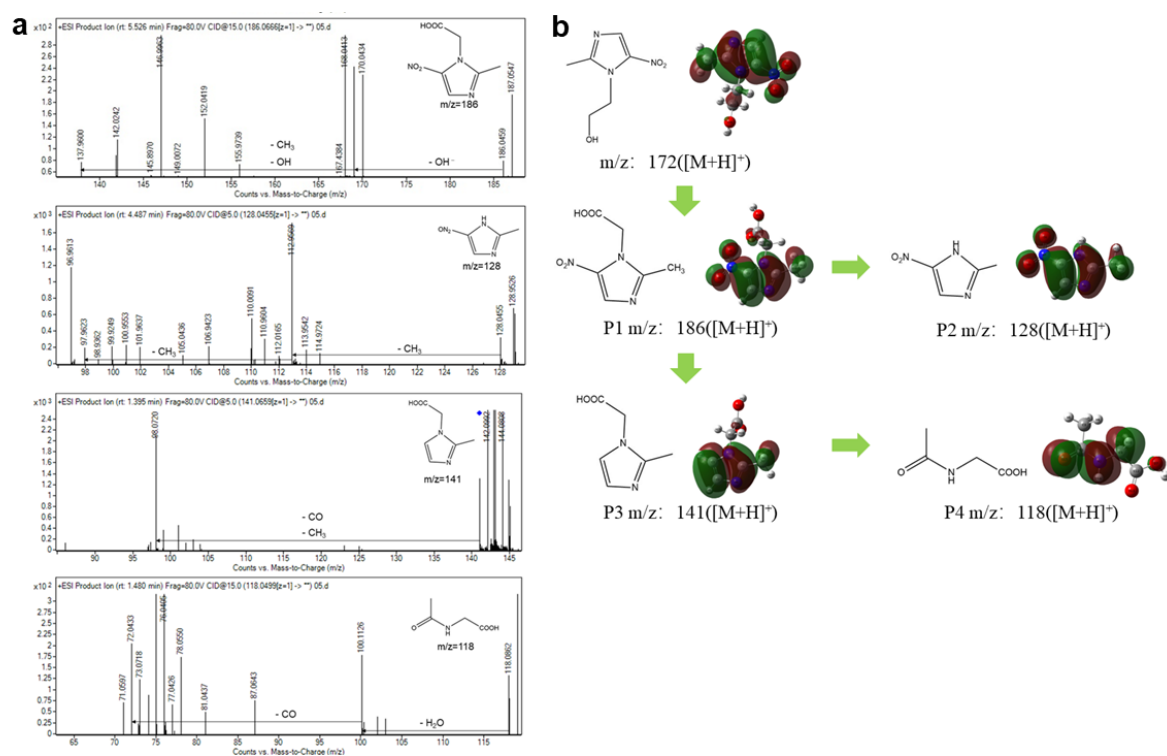


Figure S6. (a) Identification of fragment ions 186 ($[M+H]^+$), 128 ($[M+H]^+$), 141 ($[M+H]^+$), 118 ($[M+H]^+$); (b) the degradation routes in pathway I .

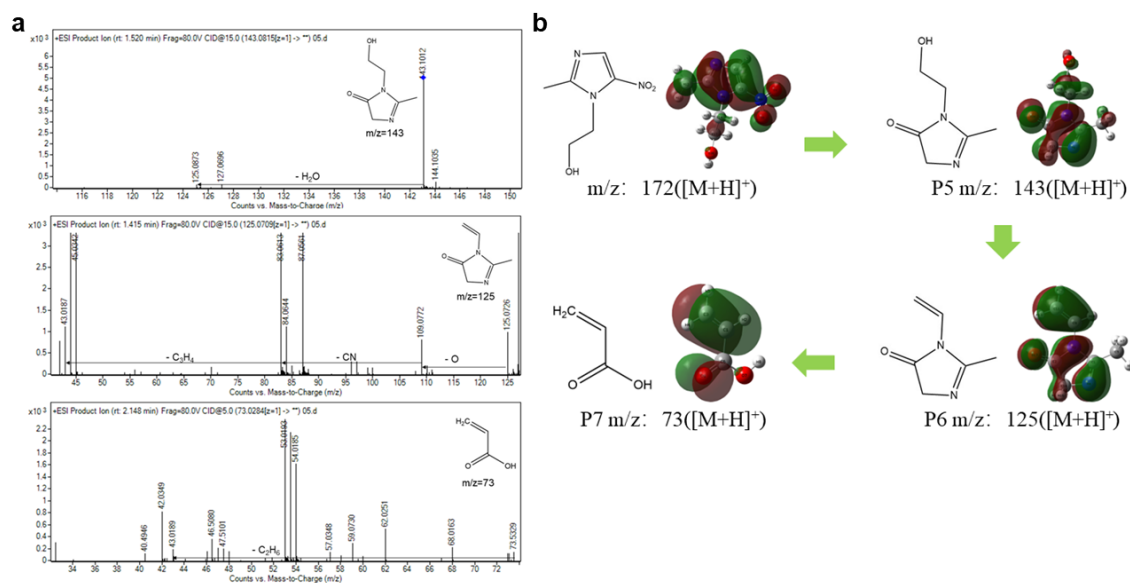


Figure S7. (a) Identification of fragment ions 143 ([M+H]⁺), 125 ([M+H]⁺), 73 ([M+H]⁺); (b) the degradation routes in pathway II .

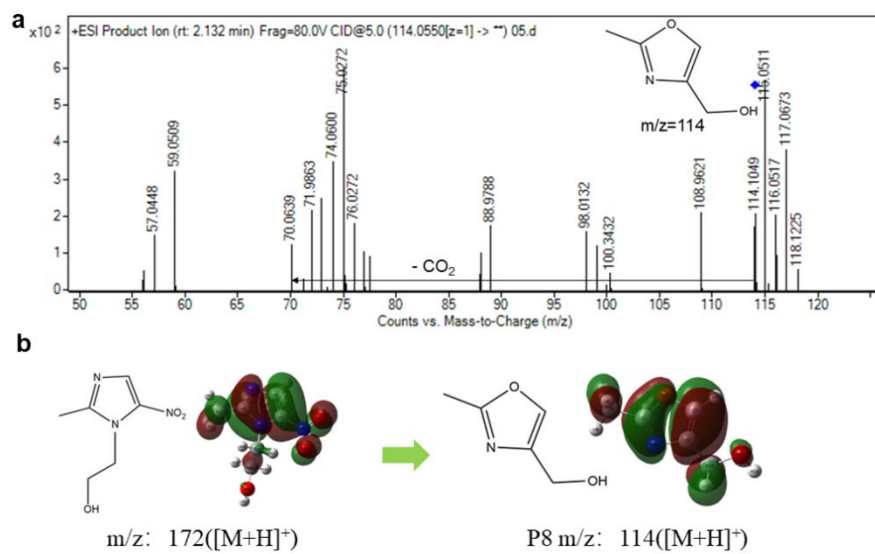


Figure S8. (a) Identification of fragment ions 114 ($[M+H]^+$); (b) the degradation routes in pathway III.

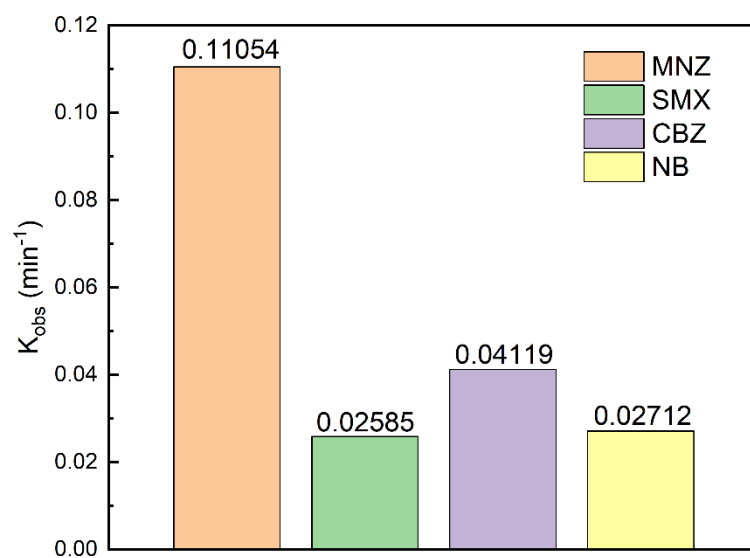


Figure S9. Pseudo-first-order kinetic constant of SMX, CBZ, NB and MNZ degradation in EC-PMS-BDD process.

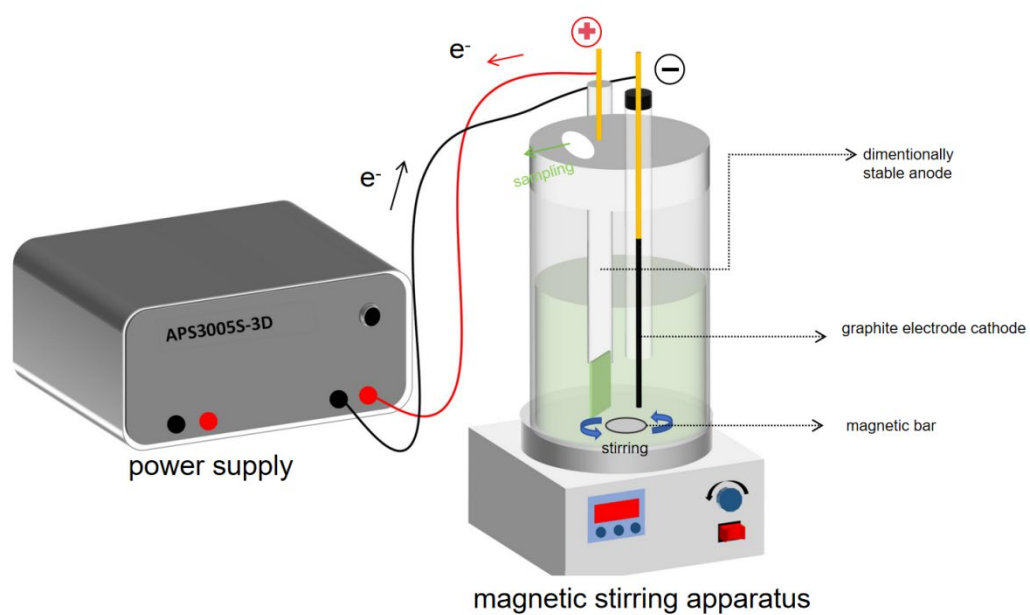


Figure S10. Schematic diagram of electrochemical oxidation system.

Table S1. Parameters of HPLC methods for analysis of different compounds.

Compound	Wavelength (nm)	Mobile phase A		Mobile phase B	
		Ultrapure Water (%)	0.1% (v/v) acetic acid solution (%)	Acetonitrile (%)	Methyl alcohol (%)
MNZ	318	80	N.A.	20	N.A.
SMX	265	N.A.	60	40	N.A.
CBZ	284	60	N.A.	40	N.A.
BA	230	50	N.A.	50	N.A.
NB	262	N.A.	50	50	N.A.
<i>p</i> -HBA/ <i>p</i> - BQ	246	70	N.A.	30	N.A.

Table S2. Actual values corresponding to coded levels of RSM.

Coded levels	A: Current density (mA/cm ²)	B: Initial pH	C: PMS dosage (mmol·L ⁻¹)	D: Reaction time (min)
-1(Low)	11.1	3	1	25
0(Medium)	22.2	6	3	35
1(High)	33.3	9	5	45

Table S3. 4-factor Box-Behnken design of RSM and experimental response.

Standard Order	Run order	Current density (mA/cm²)	Ph (1)	PMS dosage (mmol·L⁻¹)	Reaction time (min)	MNZ removal rate (1)
8	1	22.2	6	5	45	1
2	2	33.3	3	3	35	1
27	3	22.2	6	3	35	0.94103
23	4	22.2	3	3	45	1
19	5	11.1	6	5	35	0.86044
26	6	22.2	6	3	35	0.9398
22	7	22.2	9	3	25	0.74029
29	8	22.2	6	3	35	0.9407
15	9	22.2	3	5	35	0.98338
28	10	22.2	6	3	35	0.9426
3	11	11.1	9	3	35	0.76985
14	12	22.2	9	1	35	0.78515
4	13	33.3	9	3	35	0.98794
17	14	11.1	6	1	35	0.6179
11	15	11.1	6	3	45	0.79368
16	16	22.2	9	5	35	0.92868
5	17	22.2	6	1	25	0.6271
20	18	33.3	6	5	35	0.9948
18	19	33.3	6	1	35	0.9013
9	20	11.1	6	3	25	0.54074
25	21	22.2	6	3	35	0.9412
21	22	22.2	3	3	25	0.81912
12	23	33.3	6	3	45	0.99603
24	24	22.2	9	3	45	1
10	25	33.3	6	3	25	0.94412
6	26	22.2	6	5	25	0.805
13	27	22.2	3	1	35	0.84191
1	28	11.1	3	3	35	0.80368
7	29	22.2	6	1	45	0.9258

Table S4. ANOVA analysis for MNZ removal efficiency.

Source	Sum of Squares	df	Mean Square	F-Value	p-value Prob > F	
Model	0.43	14	0.031	32.24	< 0.0001	significant
A-current density	0.17	1	0.17	179.54	< 0.0001	
B-initial pH	4.648E-003	1	4.648E-003	4.84	0.0450	
C-initial PMS concentration	0.064	1	0.064	65.79	< 0.0001	
D-reaction time	0.13	1	0.13	133.92	< 0.0001	
AB	1.185E-004	1	1.185E-004	0.12	0.7305	
AC	5.553E-003	1	5.553E-003	5.79	0.0305	
AD	0.010	1	0.010	10.53	0.0059	
BC	1.061E-006	1	1.061E-006	1.106E-003	0.9739	
BD	1.554E-003	1	1.554E-003	1.62	0.2240	
CD	2.830E-003	1	2.830E-003	2.95	0.1079	
A ²	0.020	1	0.020	20.79	0.0004	
B ²	3.487E-006	1	3.487E-006	3.634E-003	0.9528	
C ²	0.015	1	0.015	15.25	0.0016	
D ²	0.021	1	0.021	22.30	0.0003	
Residual	0.013	14	9.596E-004			
Lack of Fit	0.013	10	1.343E-003	1307.41	< 0.0001	significant
Pure Error	4.109E-006	4	1.027E-006			
Cor Total	0.45	28				